Electr Eng (2010) 92:291–301
DOI 10.1007/s00202-010-0183-1

ORIGINAL PAPER

An arcless controlled switch

P. Pourmohamadiyan · K. Niayesh

Received: 4 February 2009 / Accepted: 19 October 2010 / Published online: 4 November 2010

Abstract A new current controlled switch is introduced in this paper. The switch has inherent control on the current and operates based on the motion of a conducting medium through a set of transition contacts. Basic theory concerning controlled motion of the conducting medium through a liquid metal (LM) interface is exposed followed by experimental study. The structure of the device and the design basis are described and the Lorentz force on the moving conducting medium is calculated using FEM software. Acting major role in the device operation, the forces on the conducting medium have been characterized and the motion equations of this conducting medium are solved using a numerical method. Accordingly, the design criteria, which are converted to a set of mathematical and physical constraints, are checked and the structure or quantities are modified where needed. Finally, a specimen is made and the switch operation is studied.

Keywords Current controlled switch · Arcless commutation · Liquid metal interface

1 Introduction

Many control systems have been designed to keep the system quantities in the desirable limit. Most of which, change some parameters to reach the desirable conditions through evaluation of some feedback signals. These signals are usually driven from the converted built-in quantities of the electromagnetic devices, like voltage and current. Examples of such systems can be seen in some of FACTS devices (e.g. current and voltage controlled reactors), on load tap changers (OLTC), motor starters, etc. In some of these systems, it is feasible to directly use the built-in parameters as feedback and abstain from converting parameters. Through this simplifying idea, the designer may combine or even eliminate some parts of the above mentioned system. In this paper, a new current controlled switch is introduced. The switch operates via movement of a conducting medium sliding on an LM interface. LM has been commonly used for a long time as an intermediate conducting medium [1]. Besides, its motion has also been used in some engineering applications and research areas [2–4]. Due to the type of applications, former researches mostly dealt with the steady flow characteristics of the LM [2]. LM motion has also been used in very small scale applications. Since micromachining technology was introduced in 1980s, some MEMS devices have been introduced in which micrometer sized LM droplets are actuated [5]. But due to the small size of the LM droplet and large contact angle, the motion analysis method presented in the MEMS device studies cannot be applied for high current devices. In some recent studies, considerably larger size of LM droplet has been moved to gradually change the resistance and limit the current [6,7]. In [6], the most important concern is to limit the fault current as fast as possible without any arc. In [7], the movement of the LM is not so fast because it should be controlled and settled at specific contacts when the required condition is fulfilled. Further experiments revealed that the presence of impurities and air and also constitution of metal compounds make some difficulties in smooth frequent displacement of the relatively large LM droplet.

In the present study, the LM is used as an intermediate medium to reduce the friction coefficient of the solid sliding conducting medium and the fixed contacts. Concurrently it

P. Pourmohamadiyan (✉) · K. Niayesh
School of Electrical and Computer Engineering, Campus #2, University of Tehran, PO Box 14395-515, 14395 Tehran, Iran
e-mail: pmohmad@ut.ac.ir

K. Niayesh
e-mail: kniayesh@ut.ac.ir

provides a low resistance efficient contact area between the sliding conducting medium (SCM) and the fixed contacts carrying the current. The device structure is designed based on the knowledge of constituent materials such as sliding solid conducting medium, insulation, LM and their interaction with each other. Chemical and physical properties of the LM and its contact angle are studied and the geometry of the motion path and the structure of the magnetic core are designed. An FEM solver is used to calculate the electromagnetic quantities and Lorentz force. The normal and abnormal currents of the circuit are assumed as excitations of the system. Then, motion equations of the sliding conducting medium are solved using a numerical method and the design criteria are checked in various steps. The structure or design parameters are modified where needed.

The results show that the switch can be made with dimensions of a few centimeters and can operate in the range of some 15 A of current without occurrence of undesirable phenomenon. The method introduced in this paper has several advantages compared to the conventional designs of switches, such as no need to external triggering system, much more compact sizes, no degradation of the contact system, e.g. due to the arcing and no drive mechanism. Moreover, through inherent control used in the present design, the switch does not depend on expensive auxiliary components. If different voltage sources or voltage taps with different equivalent Thevenin impedances are available, such a switch can be applied for control of load voltage. The controlled motion of the SCM may also be used in applications like motor starters, if an inexpensive method is desired.

2 Design and operation principle

Regardless of the equipment application, this paper is intended to introduce a method for arcless current commutation between contacts with known equivalent Thevenin circuits. The switch operates during transition from normal condition to abnormal condition. In our case, unacceptable voltages and currents are assumed as abnormal conditions. The current commutates between two contacts, via sliding of a conducting medium on the liquid metal wetted contacts under the effect of Lorentz force resulted from the interaction of the flowing current and a magnetic field which is also dependent on the flowing current. Figure 1 illustrates the basic scheme of the device operation and its equivalent circuit.

The parameters of the equivalent circuit shown in Fig. 1 are defined as:

- The DC currents flow through contacts A and B during equilibrium condition are denoted by I_A and I_B, respectively.

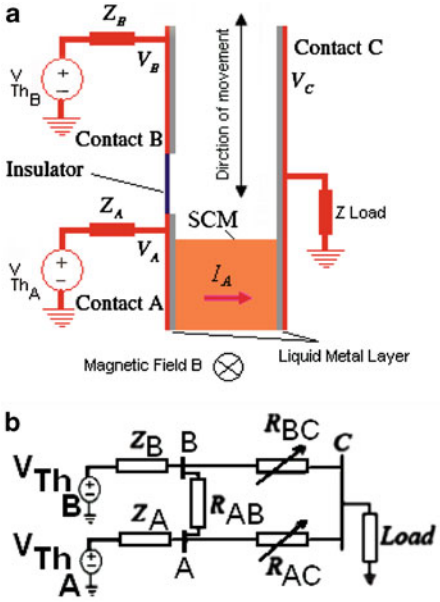

Fig. 1 **a** Basic schematics of the working principle. **b** Equivalent circuit of the device

- The nominal DC voltages of contacts A and B during equilibrium condition are denoted by V_A and V_B, respectively.
- All of the mentioned quantities during abnormal conditions (unacceptable currents and voltages), which shall lead to change over between contacts, are denoted by the same primed designation (e.g. I'_A, I'_B, etc.).
- Z_A and Z_B represent the equivalent Thevenin impedances of the sources behind contacts A and B, respectively.
- R_{Ac} and R_{BC} represent the equivalent variable resistances between the common contact C and contacts A or B, respectively. During the current commutation, one of these resistances gradually increases while the other one decreases.
- R_{AB} is the variable resistance between contacts A and B. When the system is in normal operation, this resistance is very large (almost infinity). During the current commutation and while R_{Ac} and R_{BC} are undergoing the prescribed variations, this resistance gradually decreases and reaches its minimum value. After that (when the current is completely commutated), it increases and so the contacts A and B are disconnected again.

The device has to be designed based on the following criteria:

1. The sliding conducting medium (SCM) must be remained stationary when the system quantities are in equilibrium (normal) conditions. In other words, when the system operates at acceptable voltage and current, the current shall not be commutated.

2. The SCM must start to move in a direction which will bring the system to another equilibrium condition once the system quantities reach predetermined abnormal values (threshold values of voltage and current).
3. During the commutating phase, thermal stressing must be avoided in the tail of LM and SCM. In other words, the voltage drop on these parts of circuit must be limited to a specified $u_{\max}$ (like the boiling voltage for conventional separating contacts [8]).
4. During the commutating phase, the difference between the applied voltages on the separating contacts should not exceed a minimum level $u_{\min}^{\text{arc}}$ (dependent on the contacts material [9]). Short length/duration arcs should also be prevented during separation of the SCM from LM interface of the contacts.
5. When the current completely commutates and the system reaches a new equilibrium condition, the net exerted force and the speed of the SCM must be zero.
6. The voltage appears across insulation parts should not exceed their respective breakdown voltages.

3 Device structure and forces

Due to the sliding nature of the switch contacts, a liquid metal medium is used between sliding solid conducting medium and fixed contacts. In sliding contacts, the contacting parts of the conductors slide over each other without separation. A real solid surface is not geometrically ideal because of asperities appearing during machining and subsequent use. The solid surface experiences the effects of various factors that can be classified into manufacturing, operational, and structural. These errors in form, waviness, roughness and subroughness [1] become much more important especially when two solid contacts have to slide on each other while carrying electrical current. In contacts between liquid and solid metals, the deformation of the solid member is negligible. Here, the load bearing and the apparent area are equal. Therefore, the utilization of a liquid metal as an intracontact medium separating solid contact members significantly increases the contact area encompassing almost the whole apparent area of the solid electrode surface. Hence, the electrical contact resistance and the required contact force are reduced as illustrated in Fig. 2 [10].

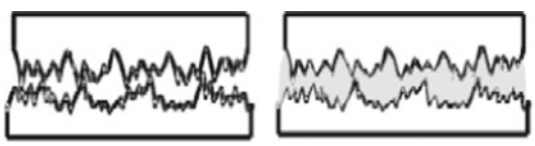

Fig. 2 *Left* Actual contact areas between two surfaces are very small, only a few points are in contact. *Right* Real contact area increases when the gap is filled with liquid metal

If a liquid metal wets the virgin surface of the solid electrode, no transition resistance occurs provided that the metals do not produce chemical compounds. When a liquid metal moistens the oxidized surface of the solid electrode surface, the contact resistance is controlled by the resistance of the oxide film, which is in the order of 10^{-9}–10^{-7} Ωm for thick oxide films. In our proposed switch, liquid metal intracontact medium does not only reduce the contact resistance and friction coefficient but also rather maintains them constant during motion of the sliding contact. This is a vital feature for the controlled motion of the sliding contact with predetermined current density, force and speed at various positions. In [11], it was concluded that interruption of metal bridges between contacts at the highest temperature point causes a metal transfer from the electrode closer to the maximum temperature of the bridge toward the other one. In such cases, the remaining stubs usually are reintegrated into the electrodes by surface tension. This is usually observed in "arcless" switching contacts. Therefore, such "bridge transfer" or "fine transfer" is considered as a major reason of "arcless" switching instead of the "arc transfer" in currents strong enough to cause obvious arcing. LM intracontact medium would likely facilitate the prescribed material transfer during switching and therefore the arcless switching is ascertained. To have a desirable form of material transfer, LM material should have low surface tension with the SCM. The sticking point in the switch operation is that the aforesaid intracontact LM medium must not move to undesired areas. Therefore, care must be taken to minimize the Lorentz force exerted on the LM particles. Hence, the current density vectors in LM particles have to be in parallel with magnetic flux density vectors affecting on the SCM. Moreover, metallurgical and chemical countermeasures have to be considered in material selection for each component. The design criteria 1, 2 and 5 of the preceding chapter imply that, at each moment, there should be a set of motive and repellent forces which interact and provide the desired conditions. As it was stated, the Lorentz force is the actuating force of the SCM. This force is proportional to the vector product of the SCM current density and a magnetic field density which is composed of two opposite components. The reference component, B_{Ref}, is generated by a coil fed by a constant reference current. This field component opposes the field generated by the control coil, B_{Cont}, which is proportional to the flowing (load) current. Hence, SCM remains stationary while the flowing current does not reach its threshold value (i.e. abnormal condition). To eliminate the direct effect of gravitational force, a horizontal path is selected for the SCM motion. Gravitational and molecular forces affect the shape and contact angle of the LM. The contact angle of the LM is determined considering the magnitude and direction of surface tension vectors. Figure 3 illustrates the general structure of the device. As it can be seen, contacts A and B are separated via a solid insulation material.

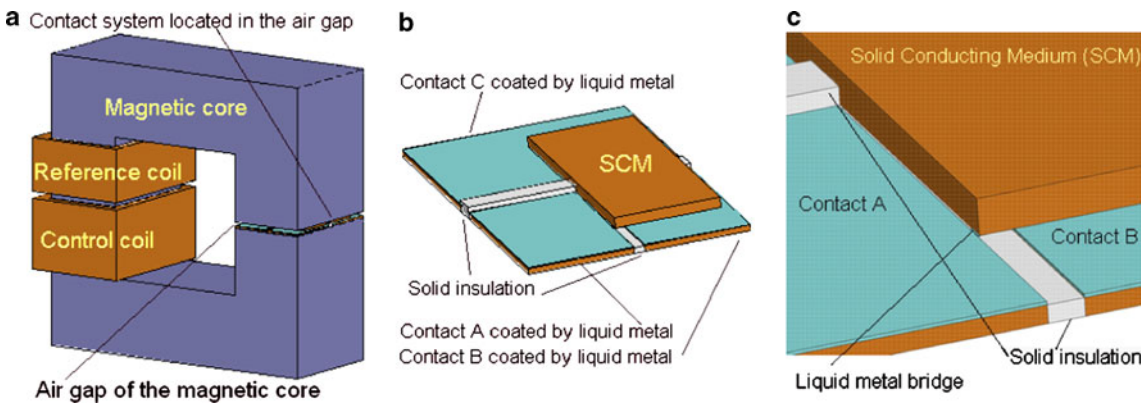

Fig. 3 Structure of the device. **a** General perspective, **b** Contact system and SCM, **c** Detail view of the contacts and the LM bridge during transition from one contact to another

To prevent any arc during contact separation, each contact has a resistance profile which facilitates the current commutation between contacts. As a result of the SCM movement, the current flowing through the second contact will gradually increase while the flowing current of the first contact decreases. The contact resistance profiles, their lengths and the distance between them should be evaluated through numerous compromises between different constraints.

The horizontal motion path of the SCM and the magnetic core which are surrounded by the reference and the control coils are designed in such way that the magnetic field density is uniform all over the motion path. Assuming a uniform distribution of magnetic field, for the first step of evaluation and design, the magnitude of Lorentz force can be estimated as:

$$\left|\vec{F}_{\text{Lorentz}}\right| = K_{\text{Device}}\,|I|\,\left|\vec{B}_{\text{net}}\right| \tag{1}$$

where

$$\left|\vec{B}_{\text{net}}\right| = \left|\vec{B}_{\text{Cont}}\right| - \left|\vec{B}_{\text{Ref}}\right| \tag{2}$$

Considering the length of the air gap encompassing the contacts system and the SCM, a linear behavior is conceivable. Hence, we have:

$$\left|\vec{B}_{\text{net}}\right| = K N_{\text{Cont}} I - K' N_{\text{Ref}} I_{\text{Ref}} \tag{3}$$

Therefore, the magnitude of Lorentz force can be expressed as:

$$\left|\vec{F}_{\text{Lorentz}}\right| = K_{\text{Device}} K N_{\text{Cont}} I^2 - K_{\text{Device}} K' N_{\text{Ref}} I I_{\text{Ref}} \tag{4}$$

where K_{Device}, K and K' are constants which depend on the system geometry. In the present design, to facilitate the control of the motion, the magnetic circuit of the device is designed in such a way that these constants almost do not change during the motion, though their small variations are also taken into account. These constants are easily determined through some simple experiments and also simulations. N_{Cont} and N_{Ref} are the number of turns of control and reference coil, respectively. The turns number or equivalent magneto motive force of each coil is determined considering the reference and threshold actuation currents and also the amount of static and dynamic friction force. To specify the optimum cross section and shape of the SCM motion path, several insulation materials and solid conducting materials with different cross sections and shapes are selected and the static and dynamic friction forces are measured through inclined plane method. In this method, the slope angle of the inclined planes are gradually increased till the SCM starts to move. Finally, the cross section which caused the motion of the SCM at least inclined plane angle is selected. Meanwhile, the insulation materials which had considerably been wetted by LM were not contributed in the design any longer. The results of the inclined plane experiments can also be used to evaluate the Lorentz force required to move the SCM. Hence, by measuring currents which actuate the SCM, the geometry dependent constants, K_{Device}, K and K', were determined. These proportionality constants are also verified through simulation by a FEM solver which calculates fields and forces.

3.1 Motion of solid conducting medium

The physical and fluid data of LM are extracted from [12] and the governing equation of motion dynamics is extracted from [13]. The motion is modeled as a solid particle drawn on the LM surface. The present research is intended to use the movement of the SCM on a thin layer of LM in a stable condition with the speeds in the order of decimeter per second. Hence, the motion dynamics of the SCM can be formulated as:

$$\begin{cases} m_{\text{SCM}} \frac{d^2 s}{dt^2} + \alpha \frac{ds}{dt} = \left|\vec{F}_{\text{EL}}\right| - \left|\vec{F}_0\right| \\ \vec{F}_0 = 0; \quad \text{when } \left|\frac{ds}{dt}\right| > 0 \end{cases} \tag{5}$$

Here, S is the position of the LM droplet and $\vec{F}_{\mathrm{EL}}$is the effective component of the Lorentz force in the direction of the motion. $\vec{F}_0$ represents the static friction force between the SCM and its surrounding medium just before movement. This force is determined through experiments and calculations and is dependent on mass and shape of the SCM. α is the loss factor, which is considered to take the velocity dependent breaking force into account. The SCM motion on the thin layer of LM, is considered to be similar to the flow around a body of the length l that is drawn through a liquid. Thus a laminar layer of LM, the so called Prandtl layer of the thickness D, occurs between the surrounding fixed contacts and the SCM:

$$D = \sqrt{\frac{6\eta l}{\rho_{\mathrm{LM}} v}} \tag{6}$$

where ρ_{LM} is the density of LM, η is the dynamic viscosity and v is the velocity magnitude of the SCM. l is the effective length of the SCM touching the LM intracontact medium in the motion path. In our device, the velocity of SCM droplet is in the range of decimeter per second, $\rho_{\mathrm{LM}} = 13{,}534\ \frac{\mathrm{kg}}{\mathrm{m}^3}$, $\eta = 0.001556\ \frac{\mathrm{kg}}{\mathrm{m\,s}}$ is the dynamic viscosity of Mercury and $l = 26$ mm is the effective length of the SCM. Accordingly, the resulting Prandtl layer is in the submillimeter range, which is smaller than LM layer thickness. Hence, the SCM is affected by a dynamic friction force $\vec{F}_{\mathrm{frict}}$

$$\left|\vec{F}_{\mathrm{frict}}\right| = \frac{\eta A v}{D} = \alpha \frac{ds}{dt} \tag{7}$$

wherein A represents the contact surface between the SCM and the LM layer. As it can be seen, this factor is dependent on the velocity of the SCM. Therefore, in order to find the exact position and velocity of the SCM, the Eq. (5) through (7) have to be solved simultaneously. For the configuration considered here, this loss factor is less than 0.0001. To verify the designed structure, the motion profile has to be checked for the condition stipulated in the design criteria. For this purpose, the start point is considered the moment at which the current flowing through contact A reaches I'_{A} (i.e. specified abnormal current of contact A). Then, using the FEM solver, the magnetic flux and current density vectors and the resulted forces components in the three Cartesian directions $\left(\vec{F}_x, \vec{F}_y \text{ and } \vec{F}_z\right)$ are calculated. In the present study, the mesh elements are built with dimensions of 0.1 mm in critical areas and number of calculation passes is set equal to twelve. Using the calculated force components, the effective components of the Lorentz force in the direction of the motion $\left(\vec{F}_{\mathrm{EL}}\right)$ can easily be calculated. The motion starts when the right hand side of Eq. (5) becomes positive. To fulfill clause 5 of the design criteria, the net exerted force and speed shall be vanished, when the SCM reaches the second equilibrium state (i.e. contact B). Moreover, through a resistance profile in the motion path, the current amplitude should be lowered enough to prevent any arc during current commutation. Since the Lorentz force depends on the flowing current and the position of the SCM, the right hand side of Eq. (5) is not constant. Thus, the motion is broken into small time steps in which the second order differential equation of (5) can be solved with constant coefficients. At the end of each time step the calculated speed $\left(\frac{ds}{dt}\big|_{t=nt_s}\right)$ and acceleration $\left(\frac{d^2s}{dt^2}\Big|_{t=nt_s}\right)$ is assumed as the initial conditions of the differential Eq. (5) which has to be solved for the next time step and position. Meanwhile, as explained earlier, the calculated speed has to be approximately checked with the presupposed α to avoid inaccurate results. The time step should be selected considering the fact that the Lorentz force changes at a rate which is dependent on the resistance profile and the hypothetical application of the proposed switch. In our method, the sampling frequency (i.e. the number of time steps per second of the motion) is much greater than twice the highest frequency of motive force variations. To assure about the successful operation of the switch, the contact angle and wettability of the LM on the solid surfaces should be evaluated. In [14], a comprehensive study has been conducted on the same materials used in relatively similar dimensions. It should also be taken into account that there are different areas in the motion path which LM has different dynamic contact angle on them.

3.2 Optimum resistance profile of the contacts

As stated, each contact has a resistance profile which facilitates the current commutation between contacts. The profiles should be determined considering three major requirements stipulated in clauses 3, 4 and 5 of the design criteria.

3.3 Thermal overstressing

During SCM motion on the resistance profile, for example different elements with different resistances, very high current densities may be reached especially in the tail of the moving particles (SCM and the LM bridge). Figure 4 illustrates the equivalent circuit of the system during transition phase of the SCM from one contact to another. To prevent thermal over stressing in the tail of LM bridge, the dissipated energy in these elements has to be kept low. The thermal overstressing of the last LM connection is equivalent to the instabilities of last connecting bridge during the contact separation in conventional switches and therefore the same formulation can be applied. So it would be possible to define a maximum voltage $u_{\max}$ (like boiling voltage for conventional separating contacts [8]), above which the last LM connection between the SCM and the wetted solid

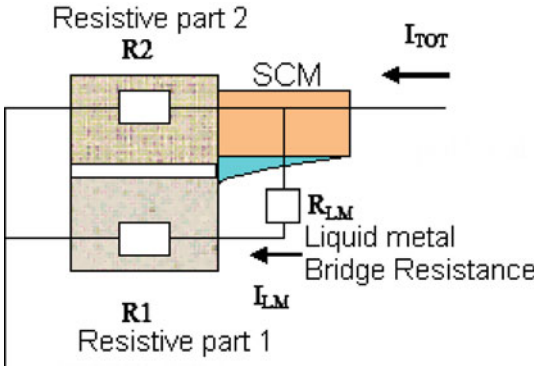

Fig. 4 Equivalent circuit of the system during SCM motion on the resistance profile elements

contact become unstable and therefore the constraint of thermal overstressing can be expressed as:

$$u_{\mathrm{LM}} < u_{\max} \tag{8}$$

where u_{LM} is the voltage drop on the LM tail that is equal to $I_{\mathrm{LM}} R_{\mathrm{LM}}$. Here, I_{LM} is current flowing through the last connection between the LM bridge and the solid electrode and R_{LM} is the resistance of the LM tail.

In [6], the equivalent circuit of similar system has been analyzed to calculate the maximum allowable R_2 for given values of R_1, R_{LM} and $u_{\max}$:

$$R_2 < \frac{R_1 + R_{\mathrm{LM}}}{\frac{R_{\mathrm{LM}} I_{\mathrm{tot}}}{u_{\max}} - 1} \tag{9}$$

Here I_{tot} is the total current flowing through LM bridge, R_1 and R_2 are the resistances of two hypothetical adjacent small elements of the resistance profile. The resistance of the LM tail, R_{LM}, is determined through experiments and also simulation of the geometry by the FEM solver.

In addition to the mentioned analytical method, to check the fulfillment of the design criteria number 3, the equivalent circuit of the device (Fig. 1b) is considered. The most difficult condition for thermal overstressing is when the thin tail of the LM is separating from the SCM and/or fixed solid contacts (see Fig. 5). Considering the Prandtl layer thickness and the speed of the motion, the worst geometry which may be occurred is simulated by the FEM solver. The resistance matrix which describes the equivalent circuit of Fig. 1 is dependent on the position of SCM and the shape of LM particles acting as bridge. The elements of this matrix are determined by applying some special cases of voltage and currents in the FEM software. Using the calculated resistances and considering the presupposed values of equivalent Thevenin voltages behind contacts, the equivalent circuit of Fig. 1b is solved. In our study, it is assumed that the resistance of the load connected to contact C is constant during current commutation. The calculated voltages and currents

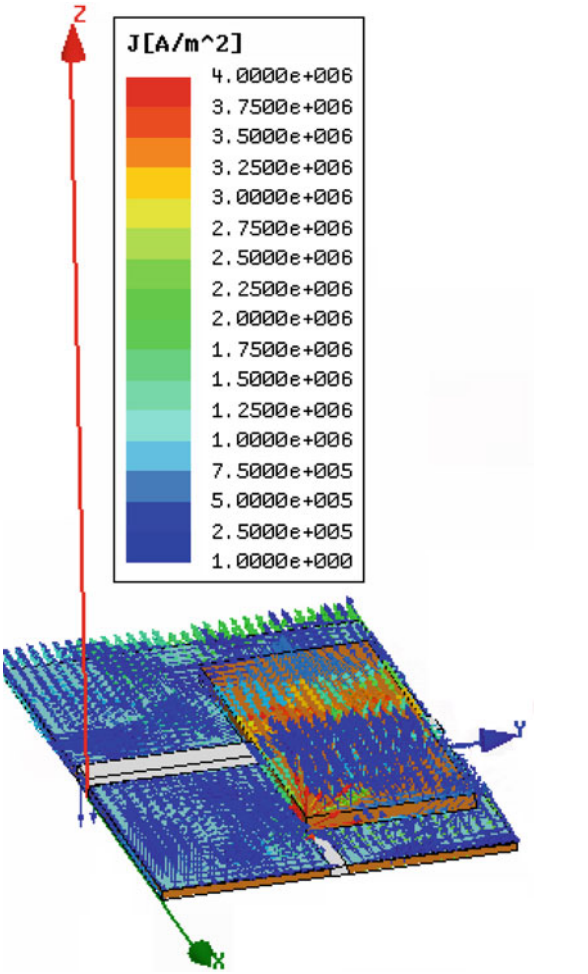

Fig. 5 Current density distribution for the worst condition during current commutation from contact A to contact B

are used as excitations of the FEM solver and the heat losses in the SCM and the LM bridge are calculated.

3.4 Arcless current commutation

3.4.1 Steady state arcs

Separation of two current carrying contacts results in initiation of switching arcs, if the voltage difference of the separating contacts exceeds a minimum level $u_{\min}^{\mathrm{arc}}$ dependent on the contact material [9]. Considering the configuration of Fig. 4, the arcless commutation constraint can be expressed as [6]:

$$R_2 < \frac{u_{\min}^{\mathrm{arc}}}{I_{\mathrm{tot}}} + R_1 \tag{10}$$

The aim of the resistance profile of each contact is to gradually reduce the contact current while the current of the other contact is increasing. But to reach the appropriate SCM motion, this reduction cannot be unlimited because the speed and transition times have to be within acceptable limits which

are compatible with the device application. Too much current reduction may cause low motive forces and subsequent failure of motion. Therefore, there is always a minimum current at the time of contact separation which will produce a voltage $V_{\text{Separation}}$ between the SCM and the LM intracontact medium left behind. The governing equation in this condition is:

$$V_{\text{Th}_\text{A}} = L_\text{A}\frac{di_\text{A}}{dt} + R(x)\,i_\text{A} + V_{\text{Separation}} + V_\text{C} \tag{11}$$

Here, V_C denotes the voltage of contact C (which is approximately equal to V_B), L_A denotes the equivalent total inductance behind contact A. $R(x)$ is the total circuit resistance when the SCM is at a distance x from the reference point. Determination of the exact value of $\frac{di_\text{A}}{dt}$ is most difficult. But it can be estimated considering the equivalent circuit and minimum transition time (maximum possible speed). During the current commutation and while the SCM is separating from the first contact, no considerable transient recovery voltage (TRV) is applied across the gap since the SCM has already been connected to the second contact. Using Eq. (11), the maximum possible value of $V_{\text{Separation}}$ is calculated. This voltage should not exceed a minimum level $u^{\text{arc}}_{\text{min}}$:

$$V_{\text{Separation}} < u^{\text{arc}}_{\text{min}} \tag{12}$$

The condition expressed in (12) should be checked when the profile is being designed based on condition of inequality of (10).

3.4.2 Arc modes of short length and duration

After progress in diagnostic techniques it has been revealed that the far known steady arc is not the only mode of arc. There are also a number of further arc modes which appear in extremely short gaps which are not stable [15]. These arc modes require minimum current and voltage values much lower than those of the steady arc discharge. Low current break arcs have to pass some of these transient modes and they may lead to the steady arc. As it was described in previous chapters, the so called "bridge transfer" is known as one way to prevent the apparent arc and ascertain "arcless switching". In our proposed design, the metal transfer in switching contacts is not too much affected by temperature as occurs in the molten metal bridge (in normal solid contacts), however, the temperature of LM bridge between SCM and fixed contacts indirectly influences the arc phenomena following contact separation.

Once the system quantities reach predetermined abnormal values (threshold values of voltage and current), SCM starts to move to connect another contact. During SCM motion, it connects to the second contact before complete separation from the first contact. As the SCM is separating from the first contact, the LM bridge diameter decreases continuously while the constriction resistance and consequently the contact voltage and the temperature in the contact constriction area increase. The LM bridge prevents contact separation due to surface tension. As the temperature inside the LM bridge increases, both viscosity and surface tension of the LM decrease. The bridge forms a catenoid. Before breakup, some small droplets may be separated from the LM bridge. Then the LM bridge becomes weak and breaks at a contact distance of about 0.1 mm. Possible disintegration of the small droplets cannot be modeled or forecasted, as it is dependent on many complicated physical conditions. But the temperature rise of the LM bridge can be estimated. The average heat power loss in the LM bridge can be expressed as:

$$P_{\text{Bridge heat loss}} = \frac{1}{T_0}\int_0^{T_0} R_\text{LM}(t)\,I^2(t)\text{d}t \tag{13}$$

where, $R_\text{LM}(t)$ is the variable resistance of LM bridge during commutation, $I(t)$ is the variable flowing current in the LM bridge and T_0 is the duration of current commutation. This time interval is selected from the moment where SCM looses its overlap with the first contact and the LM bridge is formed till the breakup moment of the bridge which is dependent on the SCM velocity. It is also possible to overestimate the LM bridge temperature rise and check the designed structure. The maximum heat power loss can be approximated assuming that maximum switching current flows through the LM bridge when the formed catenoid has the minimum possible inner diameter considering the LM properties. The geometry is modeled in the FEM solver and the maximum LM bridge resistance just before breakup $\left(R_{\text{LM}_\text{max}}\right)$ is calculated and accordingly the maximum average heat power loss is calculated. Then using Newton's law of cooling, the temperature rise of the LM bridge can be calculated with the following equation [16]:

$$q = \bar{h}\left(T_\text{body} - T_\infty\right) \tag{14}$$

where q is the total heat power generated in the LM bridge divided by the free surface area of the LM bridge (the formed catenoid), $\bar{h}$ is the average heat transfer coefficient of the body (i.e. LM bridge). T_body and T_∞ are the temperatures of the hot body and the coolant fluid, respectively (in our case the LM bridge is surrounded by air). The heat transfer coefficient of the LM $\bar{h}$, is in the range of $(3\ldots5)\cdot 10^5$ W/K m^2 [12]. The most stringent assumptions are selected to calculate the temperature rise of the LM bridge and it is observed that within the acceptable range of switch currents, the temperature rise of the bridge would not exceed 3 K. It is notable that the contribution of the thermal conduction would result in even less temperature rises. Therefore, the LM bridge temperature would not reach the boiling point of LM. Hence, no metal vapor would be present after contact separation. Therefore, thermal-field emission of electrons cannot be initiated.

In fact, the difference between melting and boiling points of LM appears as a key feature in the switch operation. The low melting point of LM facilitates the formation of the LM bridge and "metal transfer".

3.5 Forces during current commutation

The exerted forces on the SCM should be checked in each step. It is notable that there is always a difference between the Lorentz force estimated through Eq. (4) and the effective component of Lorentz force used in Eq. (5). This difference has to be determined by the FEM solver, as it is dependent on the geometry of the switch and the position of the SCM. Especially during current commutation, due to the changes of current magnitude and direction in the SCM, the ratios of Lorentz force components $\left(\vec{F}_x, \vec{F}_y \text{ and } \vec{F}_z\right)$ defer from those in normal motion of the SCM. At this critical moment, the undesirable forces must be limited to avoid irregular movement of the SCM. The calculations can be limited to critical area of concern. Another important technical point is the magnitude of the force component, which is perpendicular to the surface of the fixed contacts (in the present coordinate system that is $\vec{F}_z$). This force does not affect the motion directly, but can affect the current commutation between the SCM and fixed contacts. This force component is checked during the motion and was reduced via the change of the fixed contact shape. To have a relatively uniform Lorentz force all over the SCM volume, the magnetic field and current density distribution must be kept uniform.

Based on the requirements described for the fulfillment of the clauses 3, 4 and 5 of design criteria, a computer program is provided to check the constraints and determine the differential elements of the resistance profile of each contact. In addition to the mentioned criteria, it should not be forgotten that resistance profiles should not affect the normal operation of the system which is connected to the designed switch.

4 Experimental results

To demonstrate the described principle, a switch was designed and made with the following assumptions (according to the notations introduced for Fig. 1) to control DC voltage of load:

$V_A = 12\ \text{V},\ I_A = 13\ \text{A}$
$V'_A = 11\ \text{V},\ I'_A = 16\ \text{A}$
$V_B = 13\ \text{V},\ I_B = 18\ \text{A}$
$V'_B = 13.5\ \text{V},\ I'_B = 14\ \text{A}$
$Z_A = 0.15\ \Omega,\ Z_B = 0.05\ \Omega$

The resistance profile of the contacts A and B are designed in accordance with the procedure described in the previous chapters and Eq. 8 through 14. A compatible geometry is selected for the calculated resistance profile and the horizontal motion path. The contact areas and shapes are designed for considerably higher current density to minimize the possible temperature rise during normal operation of the switch. The fixed contacts are separated by PTFE insulation.

The intermediate liquid metal is Mercury of 99% purity. Mercury has a relatively high boiling point of about 357°C and high density which results in less evaporation and less drop scattering. These properties make this liquid metal a proper choice for intermediate contact medium though its toxicity and ecological effects should be considered for further development. Mercury also does not wet the surface of the material selected for resistance profile. If another LM material with less environmental problems is intended, the wetting effect must be checked as the most important concern. A composition of 80% Nickel and 20% Chrome is used as resistive material. The selected resistive material has resistive temperature coefficient of about $5 \times 10^{-5}\,\Omega/°\text{C}$ from 20 to 1,000°C and thermal conductivity of about 15 W/m K at 120°C. Its coefficient of linear expansion which has great importance in resistance profile design is $12.5 \times 10^{-6}/\text{K}$ from 20 to 1,000°C. Its melting temperature is 1,400°C which is much larger than maximum working temperature of the contacts. The contact angle of 1 mm diameter LM droplets on the resistor material is greater than 150°. Possible chemical reactions, especially in high temperatures, have also been studied. It was observed that no chemical reaction occurs between the LM and resistance profile when the average temperature of the interruption chamber is 175°C. Of course, in the presented sample prototype, the two latter experiments are not applicable.

The shape of SCM and the fixed contacts are designed in a manner which minimizes the number and the lengths of bounces during motion. Some simple experiments have to be done to determine the required parameters (e.g. contact angle of the LM, proportionality constant of magnetic structure, off-state resistance of the LM droplet, $\left|\vec{F}_0\right|$, etc.). The designed structure was modeled in the FEM solver. After calculation of the current density, magnetic field and forces and also simulation of SCM motion, some modifications have been done on the structure. The calculated turn numbers for reference and control coils have been modified as they are too much dependent on the magnetic core specifications, which are affected by cuttings needed for the air gap. The SCM mass has also been balanced to have a smooth motion.

The waviness, roughness and subroughness of the fixed contacts surfaces could not be well removed, but the polished surfaces of the contacts are immediately coated by LM as the oxidation will increase the contact resistances. The

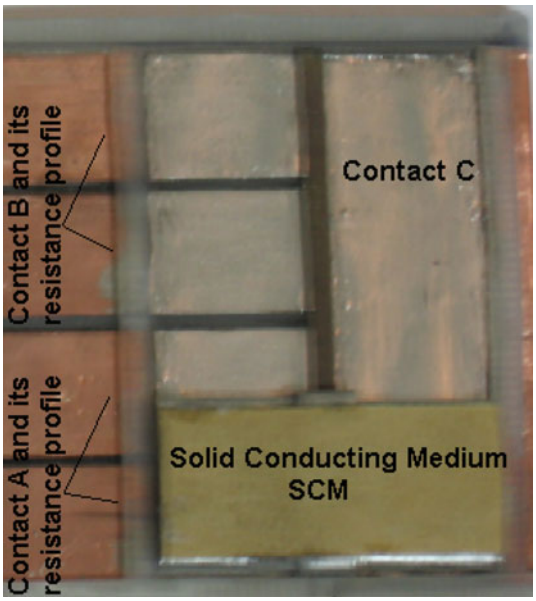

Fig. 6 Specimen to study the proposed method

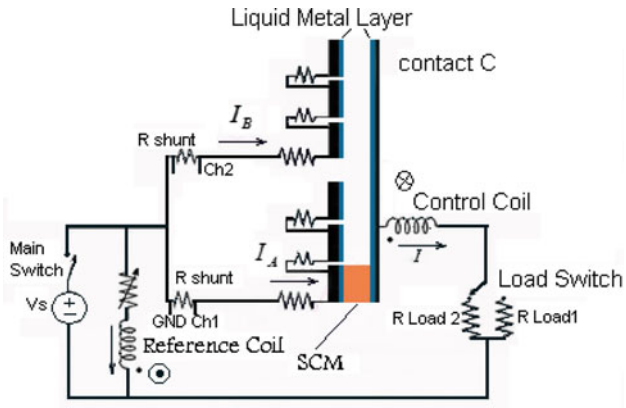

Fig. 7 Test circuit connected to the designed switch

separating insulation part is also used as a guide rail for SCM motion. The distances between the fixed solid contacts are selected based on the motion velocity of the SCM. Figure 6 shows the switch image.

The switch operation was tested in the test circuit shown in Fig. 7.

A light detector is placed in the magnetic core air gap to detect the possible arcs in the switch. The long term operation of the switch has been studied and the load voltage is recorded as main criteria of the control system. Figure 8 shows the voltage signal of the load recorded by digital oscilloscope.

As it is illustrated, during normal load current and voltage, the switch does not have any action and the SCM remains stationary between contact A and contact C. After a step change in the load (at $t = 18$ s; from R_{L1} to R_{L2}), the designed switch has compensated the load voltage drop through current

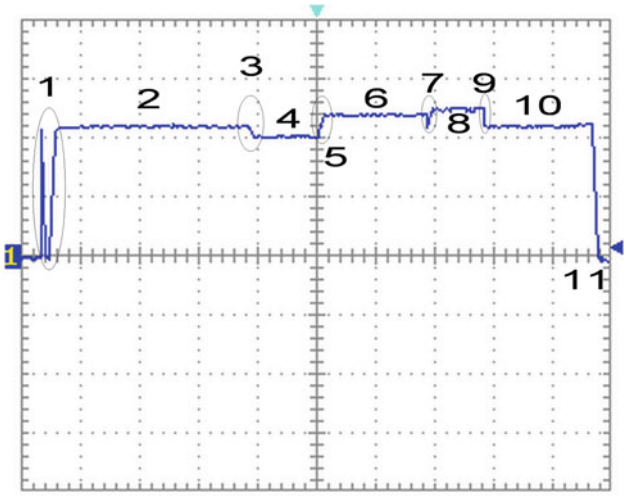

Fig. 8 Long term voltage signal of the load (5 s/div, 5 V/div, *1* arc in the main switch, *2* normal load voltage, *3* arc in the load switch, *4* abnormal load voltage after load change from RL1 to RL2, *5* controlled switching from contact A to Contact B, *6* compensated load voltage after controlled switching from contact A to contact B, *7* arc in the load switch, *8* abnormal load voltage after load change from RL2 to RL1, *9* controlled switching from contact B to contact A, *10* normal load voltage after controlled switching from contact B to contact A, *11* main switch opened)

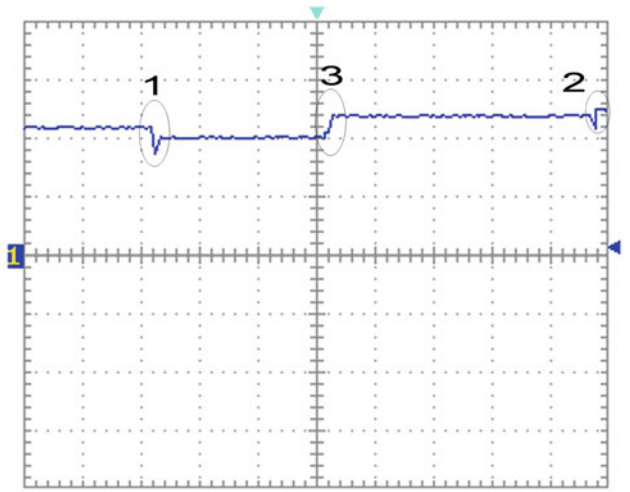

Fig. 9 Time zoom in the recorded load voltage (2 s/div, 5 V/div, *1*, *2* arc in the load switch, *3* controlled switching from contact A to contact B)

commutation to a contact with less equivalent Thevenin impedance (i.e. contact B). By changing the load to its normal value (changing the load switch position from R_{L2} to R_{L1} at $t = 38$ s), the load voltage is increased and as it is also expected the switch operates again and turns back the SCM to contact A to prevent load over voltage. To compare the switch performance with the existing commercial switches a window of the recorded load voltage is shown in Fig. 9 with smaller Time/Div.

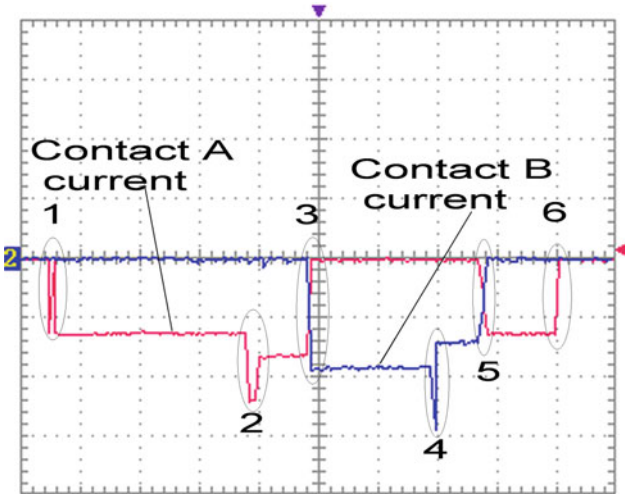

Fig. 10 Long term current signals of contacts A and B (5 s/div, 0.5 V/div, $R_{\text{Shunt}} = 0.05\ \Omega$, *1* arc in the main switch, *2* arc in the load switch from RL1 to RL2, *3* controlled switching from contact A to contact B, *4* arc in the load switch from RL2 to RL1, *5* controlled switching from contact B to contact A, *6* main switch opened)

As it can be seen during load step changes, two voltage dips have occurred which are caused by the arc voltage drop in the load switch. But the designed switch operation hasn't caused any similar voltage dip though it has compensated the load voltage with considerable delay.

In another test, the switch currents have been recorded via two similar shunt resistances of 0.05 Ω. As shown in Fig. 10, the load current flowing through contact A is suddenly increased due to a step change in the load (from R_{L1} to R_{L2}) the arc in the load switch can be well recognized. The current commutations from contact A to contact B and vice versa are also marked. As it is illustrated, the current has been commutated between two switch contacts without any arc.

The long duration needed for the switch operation is mainly caused by the length of the resistance profiles of each contact. This problem could be solved if the resistance profile could be made with smaller segments. If so, the SCM dimension and mass could also be decreased. The delayed operation is also caused by the speed profile needed for smooth operation of the device. According to the design criteria, the speed of the SCM and the net force exerted on it must vanish when it reached the final position (contact B). To solve this problem, the applied motive force (Lorentz force) could be increased and the stoppage of the SCM could be done by mechanical means. This in effect, increases the average velocity of the SCM and decreases the time needed for the switch operation. But this remedy cannot be generalized for switches with higher number of contacts as stoppage at middle way contacts is a major requirement according to the design criteria.

5 Conclusions

This paper presents a method for arcless controlled current commutation. The working principle of the proposed device is based on the motion of a solid conducting medium on the liquid metal wetted contacts under the influence of Lorentz force. The phenomena relating to the current commutation have been investigated and the relevant theoretical constraints have been derived. The electromagnetic quantities for each time step of the SCM motion have been calculated by a FEM solver and the motion equations are solved by a numerical method. Based on the simulation results, some modifications have been done on the design parameters. Then, a specimen has been made to study the proposed method. The experimental results indicate that no arc occurs during current commutation though the operation speed is not high enough. Some countermeasures have been proposed to increase the operation speed. The switch takes advantage of the controllable arcless operation without external triggering, with relatively small size. Moreover, due to the liquid metal layer on the contacts, some usual problems of conventional switches like surface degradation of contacts and mal-operation of mechanical mechanisms can be avoided.

Acknowledgments This work was supported by Iran National Science Foundation through Grant No. 86064/26.

References

1. Braunovic M, Konchits V, Myshkin NK (2006) Electrical contacts; fundamentals, applications and technology. Taylor & Francis Group, LLC
2. Takahashi M, Momozaki Y (2000) Pressure drop and heat transfer of a mercury single-phase flow and an air–mercury two-phase flow in a helical tube under a strong magnetic field. Fusion Eng Des 51–52:869–877
3. Davidson PA (2001) An introduction to magnetohydrodynamics. Cambridge University Press, Cambridge
4. Smolentsev S, Abdou M (2005) Open-surface MHD flow over a curved wall in the 3-D thin-shear-layer approximation. Appl Math Model 29:215–234
5. Latorre et al (2002) Electrostatic actuation of microscale liquid–metal droplets. J MEMS 11(4):302–308
6. Niayesh K, Tepper J, Koenig K (2006) A novel current limitation principle based on application of liquid metals. IEEE Trans Compon Packag Technol 29(2):303–309
7. Pourmohamadiyan P, Niayesh K (2008) Conceptual design of a novel arcless controlled switch. doi:10.1007/s00202-008-0104-8
8. Slade P (1999) Electrical contacts: principals and applications. Marcel Decker Inc., New York
9. Holm R (2000) Electric contacts: theory and applications, 4th edn. Springer Verlag, Berlin, Germany
10. Cao A, Yuen P, Lin L (2007) Microrelays with bidirectional electrothermal electromagnetic actuators and liquid metal wetted contacts. IEEE J MEMS 16(3):700–708
11. Fairweather A (1945) The closure and partial separation of a metallic contact. In: Proc IEE Part I, vol 92, p 92

12. Cord H (1998) A literature survey on fluid flow data for mercury-constitutive equation. European Spallation Source (ESS), paper 81-T
13. Schoft S, Tepper J, Niayesh K (2005) Short circuit current limitation by means of liquid metal technology. Proc 10th Int Conf. Switching Arc Phenomenon, Lodz, Poland, pp 187–196
14. Awasthi A et al (1996) Measurement of contact angle in systems involving liquid metals. Meas Sci Technol, pp 753–757
15. Rieder WF (2000) Low current arc modes of short length and time: a review. IEEE Trans Compon Packag Technol 23(2):286–292
16. Leinhard JH (2006) A heat transfer textbook, 3rd edn. Phlogiston Press, Cambridge, Massachusetts, USA